Aggregates Formed by Amphoteric Diblock Copolymers in Water

Jean-François Gohy,[†] Serge Creutz,[†,§] Myriam Garcia,[†,⊥] Boris Mahltig,[‡] Manfred Stamm,[‡] and Robert Jérôme*[,†]

Center for Education and Research on Macromolecules (CERM), Institute of Chemistry B6, University of Liège, Sart-Tilman, B-4000 Liège, Belgium, and Max-Planck-Institut für Polymerforschung, Ackermannweg 10, 55128 Mainz, Germany

Received December 1, 1999; Revised Manuscript Received May 22, 2000

ABSTRACT: The associating behavior of a series of monodisperse poly(2-(dimethylamino)ethyl methacrylate)-*b*-poly(methacrylic acid) (PDMAEMA-*b*-PMAA) ampholytic diblock copolymers has been studied in water in the dilute regime as a function of pH and salt concentration. Dynamic light scattering (DLS) has been used to monitor the association behavior and transmission electron microscopy (TEM) to visualize the morphology of the aggregates. At and around the isoelectric point (IEP) of the ampholytic diblocks, strong electrostatic interactions occur and lead to the formation of insoluble complexes between negatively and positively charged blocks. These electrostatic interactions can be screened by the addition of salt, which leads to the partial dissolution of the material, according to Debye screening. For samples containing a major PDMAEMA block, spherical micelles are observed below the IEP. These micelles consist of a PMAA core surrounded by a water-soluble protonated PDMAEMA corona. At and above the IEP, these samples are insoluble. Spherical micelles are also formed below the IEP for samples containing a minor PDMAEMA block. These copolymers are insoluble at and around the IEP, whereas solubility is observed above the IEP with formation of aggregates of remarkable morphologies, including hollow spheres and complex compartmentalized aggregates. This aggregation is most favorable at high pH, and it cannot be accounted for only by electrostatic interaction between oppositely charged blocks. Indeed, short-range hydrophobic interaction between uncharged PDMAEMA blocks seems to play a key role in the association process. This is emphasized by quaternized poly(2-(dimethylamino)ethyl methacrylate)-*b*-poly(methacrylic acid) ampholytic copolymers which are carrying a permanent positive charge on the aminated monomeric units and do not form these particular aggregates.

Introduction

The association of amphiphilic block copolymers dissolved in a selective solvent of one constituent is well documented in the scientific literature.[1] In most cases, spherical aggregates are formed, which consist of a core formed by the insoluble blocks surrounded by a shell formed by the solvated blocks. The number of block copolymers chains in a micelle (Z) as well as the related size of the micelles can be predicted by general relationship (eq 1) for many systems, including strongly segregated diblock, triblock and graft copolymers, low molecular weight nonionic, and anionic and cationic surfactants.[2]

$$Z = Z_0 N_A^{\,2} N_B^{\,-0.8} \qquad (1)$$

where N_A and N_B are the degree of polymerization of the insoluble block and the soluble block, respectively, and Z_0 is a parameter related to the interaction parameter between the constitutive blocks and the packing parameter introduced by Israelachvili.[3]

In recent years, other types of supramolecular organization including rods, lamellae, vesicles, and tubules were observed for the amphiphilic block copolymers.[4] These structures are entropically driven, whenever the chains of the core-forming blocks are less stretched than in dense spherical aggregates. Eisenberg et al. reported on the formation of the so-called "crew-cut" aggregates, formed by highly asymmetric diblock copolymers consisting of a short hydrophilic polyelectrolyte or neutral block and a long hydrophobic polystyrene or polybutadiene block.[4,5] These aggregates were actually formed by the addition of a small amount of water to the copolymer dissolved in a nonselective solvent, e.g., dimethylformamide. They were kinetically frozen in by the addition of a large excess of water followed by the removal of the nonselective solvent by dialysis. Other strategies were also reported for the formation of nonspherical copolymer micelles. Vesicle-like aggregates were directly prepared by dissolution of diblocks in organic solvents selective for one block.[6] These structures were further stabilized by the cross-linking of the insoluble blocks. Selective degradation of the soluble block resulted in shaved or semishaved vesicles.[7] Another technique to produce hollow aggregates consists of using amphiphilic rod−coil copolymers, as shown by Jenekhe and Chen.[8] In this case, large hollow cavities were formed as result of the unability of the large rigid block to pack into dense spherical cores. A variety of supramolecular organizations were also observed for amphiphilic copolymers containing a polystyrene block and a charged poly(isocyanide) block derived from isocyano-L-alanine-L-alanine and isocyano-L-alanine-L-histidine.[9] The chirality of these copolymers allows spectacular helical superstructures to be formed in addition to vesicles. Giant vesicles were also reported in the case of a low molecular weight poly(ethylene oxide)-*b*-poly(ethylethylene) copolymer, which was prone to form lamellar phase in water over a broad range of concentrations and temperatures.[10] The mechanical

[†] University of Liège.
[‡] Max-Planck-Institut für Polymerforschung.
[§] Present address: Dow Corning, Parc Industriel, B-7180 Seneffe, Belgium.
[⊥] Present address: EXXON, Hermeslaan 2, B-1831 Machelen, Belgium.
* To whom correspondence should be addressed.

10.1021/ma992016j CCC: $19.00
Published on Web 08/03/2000

Table 1. Molecular Characteristic Features of the Samples Considered in This Study

sample: PMAA(x)-*b*-PDMAEMA(y)[a]	$\bar{M}_n$ PMAA block	polydispersity of the PMAA block	$\bar{M}_n$ copolymer	polydispersity of copolymer	composition (wt % DMAEMA)	IEP[b]	IEP[c]	IEP[d]
PMAA(15)-*b*-PDMAEMA(120)	1300	1.20	20100	1.09	93	8.9	8.9	8.9
PMAA(51)-*b*-PDMAEMA(109)	4400	1.06	21500	1.12	79	7.6 ± 0.5	8.1	8.0
PMAA(49)-*b*-PDMAEMA(11)	4200	1.10	5900	1.10	29	5.4 ± 0.6	4.8	5.0
PMAA(49)-*b*-PDMAEMA(23)	4200	1.10	7800	1.10	46	5.9 ± 0.7	5.3	5.5

[a] *x* and *y* are the degrees of polymerization of the PMAA and PDMAEMA blocks, respectively. [b] IEP determined by zeta potential measurements. [c] IEP calculated from eq 8. [d] IEP determined by the isoionic method.

properties of these giant vesicles were found to be almost an order of magnitude tougher than the classical lipid membranes.

This paper aims at reporting on the supramolecular organization of another class of copolymers, i.e., amphotheric block copolymers, particularly a series of poly(2-(dimethylamino)ethyl methacrylate)-*b*-poly(methacrylic acid) (PDMAEMA-*b*-PMAA). Depending of the pH of the aqueous solution, the DMAEMA units can be positively charged and the MAA units be neutral, the MAA units can be negatively charged and the DMAEMA units be neutral, and finally the two blocks can be charged, thus leading to a polyampholytic copolymer. At the isoelectric point, there are as many positive charges as negative charges.

The electrostatic interaction of the oppositely charged blocks is expected to be an additional driving force to the aggregation of the PDMAEMA-*b*-PMAA diblocks. Actually, this strategy was recently used by Kataoka et al. to produce monodisperse spherical aggregates merely by mixing poly(ethylene oxide)-*b*-poly(α,*β*-aspartic acid) with oppositely charged poly(ethylene oxide)-*b*-poly(L-lysine) diblocks.[11] These authors showed that chain length recognition occurs, the supramolecular assembly being the result of the association of oppositely charged blocks of equal length. Cohen-Stuart et al.[12] also used electrostatic interactions in order to build up a micellar core, based on the fact that a micelle can be regarded as a small droplet of a new phase that has been arrested in its growth because part of the constituent molecules does not participate in the phase separation but remains in contact with the solvent. In this case, the phase separation was induced by the electrostatic interaction of oppositely charged polymers. The micellar aggregates were actually formed by mixing a water-soluble polyanion and a diblock copolymer consisting of two water-soluble blocks: one cationic and one neutral. In this paper, two series of PDMAEMA-*b*-PMAA copolymers will be studied, the PDMAEMA block being the major in the first series and the minor constituent in the second series.

Experimental Section

Polymer Synthesis. The diblock copolymers were anionically synthesized as reported elsewhere.[13] Briefly, the monomers were purified by distillation over triethylaluminum. The glass reactor containing the required amount of LiCl (10/1 LiCl/initiator molar ratio) was flamed-dried under vacuum, purged with nitrogen, added with the solvent (tetrahydrofuran), and cooled to −78 °C. Diphenylmethyllithium was added dropwise until a persistent yellow color was observed, followed by the required amount of this initiator. *tert*-Butyl methacrylate was first polymerized at −78 °C for 1 h, followed by DMAEMA (2 h at −78 °C). A sample was picked out from the reactor before the addition of DMAEMA. The copolymerization reaction was then quenched with methanol. The characterization of the products was performed by size exclusion chromatography (SEC) and nuclear magnetic resonance (NMR). SEC was performed in tetrahydrofuran added with 1% (v/v) triethylamine, using a Hewlett-Packard 1050 liquid chromatograph equipped with two Plgel columns (1000 and 10 000 Å, respectively) and a Hewlett-Packard 1047A refractive index detector. Poly(methyl methacrylate) standards were used for calibration. ^{1}H NMR spectra were recorded at 400 MHz with Bruker AM 400 spectrometer. $\bar{M}_n$ of the second block was calculated from the ^{1}H NMR spectrum of the copolymer and $\bar{M}_n$ of the first block. The *tert*-butyl methacrylate units were converted into methacrylic acid (MAA) by hydrolysis at the reflux of dioxane/HCl 9/1 v/v for 2 days. The final (co)polymers were purified by dialysis against regularly replaced distilled water for 2 weeks, and they were thought to be "neutral" when recovered.

The PDMAEMA block of the copolymers was quaternized by iodomethane. In a typical experiment, the PMAA-*b*-PDMAEMA diblock was dissolved in methanol and added with an excess of iodomethane (5/1 CH_3I/DMAEMA molar ratio). The solution was refluxed for 4 days, and the quaternized product was purified by dialysis against distilled water. The final copolymers were finally recovered by gentle evaporation of water. The molecular characteristics of all the copolymers analyzed in this study are listed in Table 1.

Preparation of the Copolymer Solution. A 1 wt/vol % stock solution of each copolymer in water was prepared. This solution was further diluted to 0.01 wt/vol % in glass vessels containing pH- and ionic strength-adjusted water. pH was fixed by using 50 mM phosphate buffer. NaCl was used to adjust the ionic strength, when required. In all the experiments, bidistilled water was used and was filtered through 0.2 μm syringe filters.

Dynamic Light Scattering (DLS). DLS measurements were performed with a Brookhaven Instruments Corp. DLS apparatus that consists of a BI-200 goniometer, a BI-2030 digital correlator, and an Ar ion laser (LEXEL Lasers) with a wavelength of 488 nm. The scattering angle used for the measurements was 90°. A refractive index matching bath of filtered decalin surrounded the scattering cell, and the temperature was controlled at 25 °C. Prior to sample loading, appropriate glass vessels were soaked overnight in sulfochromic solution, thoroughly cleaned with bidistilled water, and dried in a vacuum oven.

The experimental correlation function $G_2(t)$ was measured. For a single-exponential decay, $G_2(t)$ can be expressed by eq 2:

$$G_2(t) = B[1 + \beta \exp(-2\Gamma t)] \quad (2)$$

where B is the baseline, β is an optical constant that depends on the instrument, and Γ is the decay rate for the process, t being the time This rate is given by

$$\Gamma = Dq^2 \quad (3)$$

where D is the translation diffusion coefficient and q is the absolute value of the scattering vector

$$q = [4\pi n \sin(\theta/2)]/\lambda \quad (4)$$

n is the refractive index of the solvent, θ is the diffusion angle, and λ is the wavelength of the incident light.

The diffusion coefficient extrapolated to zero concentration (D_0) for spherical particles is related to the hydrodynamic radius R_h by the Stokes−Einstein equation:

$$D_0 = k_B T/6\pi\eta R_h \quad (5)$$

where k_B is the Boltzmann constant, T is the absolute temperature, and η is the viscosity of the solvent.

When aggregates of different sizes are formed in solution, the experimental correlation function depends on all the individual decay processes. In this case, the data analysis was performed using the CONTIN routine, a constrained regularization method program for the inverse Laplace transformation of dynamic light scattering data. The CONTIN program can give access to the distribution of the relaxation times in the experimental time correlation functions. The *Z*-averaged distribution of R_h was then calculated.

Transmission Electron Microscopy (TEM). TEM observations were carried out with a Philips CM 100 operating at a voltage of 100 kV. A Gatan 673 CCD camera was used to directly record the TEM pictures which were then transferred to a computer equipped with the Kontron KS 100 software.

Samples were prepared by dipping Formvar-coated copper TEM grid into the copolymer water solution ($C = 0.01$ wt/vol %). The grid was then immediately frozen in liquid nitrogen, and water was lyophilized. After half an hour of lyophilization, the grid was inserted in the microscope for observation. This method is suitable for the observation of diluted solutions.

Concentrated copolymer solutions were occasionally studied by cryo-TEM. Cryo-TEM observations were performed with a Philips CM12 operating with a 120 kV acceleration voltage at −170 °C. Thin films were prepared by dipping a 700 mesh copper grid in the copolymer solution ($C = 10$ wt/vol %). The solution excess was removed with a filter paper. The sample was quenched at the freezing point of liquid ethane. The vitrified specimens were stored under liquid nitrogen and subsequently transferred to the electron microscope using a Gatan 626 cryotransfer system.

Fluorescence Spectroscopy. Steady-state fluorescence measurements were carried out with a Perkin-Elmer LS 50 apparatus at room temperature. Pyrene was used as a probe of the hydrophobic domains. Pyrene was first recrystallized in absolute ethanol. A stock solution of pyrene in chloroform was then prepared ($C = 2 \times 10^{-5}$ mol/L). A 100 μL aliquot of this solution was poured into a glass vessel, and chloroform was evaporated. A 2 mL aliquot of a 1 w/w % water solution of the copolymer were added. The contents of the vessels were stirred for at least 24 h before analysis.

The excitation wavelength (λ_{ex}) was 335 nm. The experimental data were the average of three independent measurements, with a standard deviation lower than 3%.

Electrophoretic Mobility. A Coulter DELSA 440 was used for the measurement of the electrophoretic mobility by a light scattering technique. As a result of the Doppler effect, the frequency of the scattered laser light is different from the frequency of the original laser beam. This frequency shift is related to the particle velocity. The relationship between the frequency shift and the electrophoretic mobility is expressed by the following equation:

$$U = (\nu_d \lambda)/[2En \sin(\theta/2)] \quad (6)$$

where ν_d is the frequency shift, U is the electrophoretic mobility, and E is the electrical field strength.

The zeta potential is related to the electrophoretic mobility by eq 7.

$$U = \frac{\epsilon\xi}{\eta} \quad (7)$$

where ϵ is the dielectric constant and ξ is the zeta potential.

Zeta potential measurements were carried out in 100 mmol NaCl solutions in order to keep a constant electrical double layer.

Results and Discussion

The data collected for the two PMAA(15)-*b*-PDMAEMA(120) and PMAA(49)-*b*-PDMAEMA(11) diblocks will be essentially reported, with some references to the PMAA(49)-*b*-PDMAEMA(23) and PMAA(51)-*b*-PDMAEMA(109) copolymers. Indeed, the general behavior of the PMAA(15)-*b*-PDMAEMA(120) and PMAA(51)-*b*-PDMAEMA(109) samples is basically the same, which is also the case for the PMAA(49)-*b*-PDMAEMA(23) and PMAA(49)-*b*-PDMAEMA(11) diblocks.

Table 2. Zeta Potential Measured for the PMAA-*b*-PDMAEMA Copolymers at Different pHs Values ($C = 0.01$ wt/vol %)

pH	ζ (mV) PMAA(49)-*b*-PDMAEMA(11)	ζ (mV) PMAA(15)-*b*-PDMAEMA(120)
2	+26.1 ± 3.2	+39.2 ± 5.7
4	+14.2 ± 1.5	+37.3 ± 1.7
6		+28.4 ± 2.5
8	−34.4 ± 1.7	+2.1 ± 1.8
10	−57.8 ± 2.8	−42.6 ± 1.6

Electrophoretic Mobility and Isoelectric Point. The electrophoretic mobility of the 0.01 wt % water solution of each copolymer considered in this study has been measured as a function of pH. At pHs smaller than the IEP, the aggregates formed by the ampholytic PMAA-*b*-PDMAEMA diblocks have a net positive charge. At the IEP, the net charge is zero, and it turns to a negative value at pHs higher than the IEP, as exemplified in Table 2. The IEP is however not clearly detected for most of the copolymers, as result of their insolubility in the vicinity of this particular pH. As a crude approximation, the IEP has been considered as the value at the midpoint of the pH range of insolubility (Table 1).

The IEP has been also determined by the so-called isoionic point method described by Patrickios et al.[14] This method simply consists of measuring the pH of a 10 wt % suspension of neutral PMAA-*b*-PDMAEMA copolymer, after equilibration in deionized water. This isoionic pH is considered to be the IEP.[15] Patrickios et al. found a good agreement between the IEP as determined by the isoionic pH and the midpoints of the pH range of precipitation.[14] The isoionic points of the samples are listed in Table 1 and are more reliable values for IEP, because they were measured in the absence of salt, which may interact with the polyampholyte, thus leading to a shift in IEP or the pH region of precipitation.[16,17] The IEP has also also calculated by using eq 8, based on the requirement that the net charge of the polyampholyte is zero and that the dissociation constants are not composition dependent.[14,18,19]

$$\mathrm{IEP} = \mathrm{p}K_{a,\mathrm{PDMAEMA}} + \log\left\{\frac{1}{2}\left[\frac{1-R}{R} + \left(\left(\frac{1-R}{R}\right)^2 + \frac{4}{R}\,10^{\mathrm{p}K_{a,\mathrm{PMAA}}-\mathrm{p}K_{a,\mathrm{PDMAEMA}}}\right)^{1/2}\right]\right\} \quad (8)$$

According to this equation, IEP depends on the acid to base molar ratio, R, and the dissociation constants $\mathrm{p}K_{a,\mathrm{PMAA}} = 5.35$[20] and $\mathrm{p}K_{a,\mathrm{PDMAEMA}} = 8$.[14] The accordingly calculated IEP values are listed in Table 1. A fairly good agreement is noted between these values and the isoionic pHs.

It must be noted that a value of 6.6 has also been reported for $\mathrm{p}K_{a,\mathrm{PDMAEMA}}$.[21−23] This unusually low value was thought to result from the cyclization of the side-chain conformation such that the amine group is stabilized by the carbonyl of the side chain.[21] In the present study, the $\mathrm{p}K_{a,\mathrm{PDMAEMA}}$ value of 8 is expected

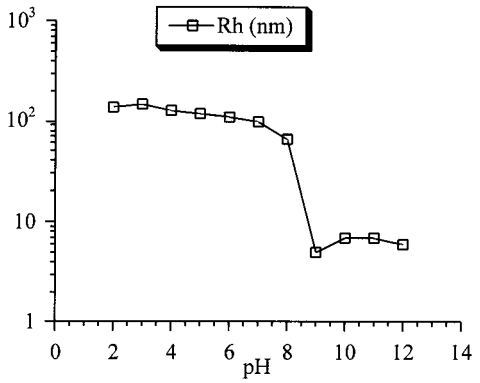

Figure 1. Hydrodynamic radius of the aggregates formed by the PMAA(15)-*b*-PDMAEMA(120) copolymer as a function of pH (C = 0.01 wt/vol %).

to be more reliable because the stability of the cyclic conformation in the presence of the phosphate buffer salt is very questionable. Moreover, Pradny and Seveik have shown that the PDMAEMA homopolymer becomes more acidic as the degree of protonation increases because of mutual repulsion of the positive charges along the chains.[21] The charges along the polymer are screened by the salt, which increases the effective pK_a of PDMAEMA.

Dynamic Light Scattering (DLS). The sizes of the micelles and their distribution have been measured by DLS, at several salt concentrations and pHs. The effect of copolymer concentration on micelle size has been found to be negligible and will not be discussed in the following. Actually, a quite monotonic decrease in the scattered intensity is actually observed at decreasing concentration, which has been used elsewhere to determine the critical micellar concentration.[24] On the basis of DLS results, the PMAA-*b*-PDMAEMA copolymers fall into two categories: the copolymers with a major PMAA block and those ones containing a major PDMAEMA block.

The PMAA(15)-*b*-PDMAEMA(120) copolymer is a typical example of diblocks containing a major PDMAEMA block. Figure 1 shows that below the IEP, which is located at pH = 8.9 (Table 1), micelles are formed that consist of a PMAA core surrounded by a charged PDMAEMA shell. A slight decrease of the micelle size is observed upon increasing pH, more likely as a result of the decreased electrostatic repulsion of the charged PDMAEMA chains in the corona, which tends to reduce the stretching of these chains and thus the size of the micelles. At and above the IEP, the copolymer becomes insoluble. This is thought to result from hydrophobic interactions between uncharged PDMAEMA blocks that render the copolymer insoluble. That hydrophobic interactions are operative is confirmed by the fact that addition of salt does not restore solubility. Small aggregates are however detected by DLS in the supernatant at and above the IEP. They are not observed for the PMAA(51)-*b*-PDMAEMA(109) copolymer. The CONTIN size distribution of the micelles formed by the PMAA(15)-*b*-PDMAEMA(120) copolymer at different pHs is shown in Figure 2.

The behavior of the quaternized PMAA(15)-*b*-PDMAEMA(120) copolymer is quite similar to that one of the nonquaternized sample as shown by the comparison of Figures 1 and 3. Since the major block of this copolymer is the quaternized PDMAEMA block, an excess of positive charges is always present in this

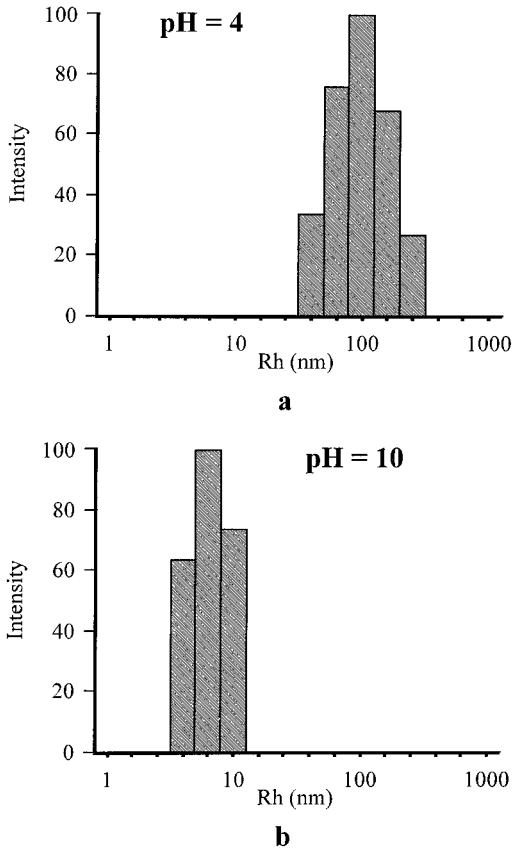

Figure 2. CONTIN size distribution for the PMAA(15)-*b*-PDMAEMA(120) copolymer at pH = 4 (a) and pH = 10 (b) (C = 0.01 wt/vol %).

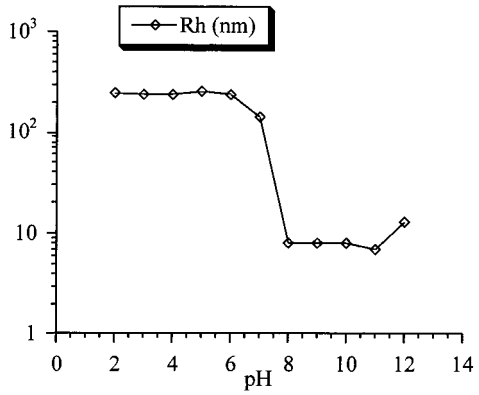

Figure 3. Hydrodynamic radius of the quaternized PMAA-(15)-*b*-PDMAEMA(120) copolymer as a function of pH (C = 0.01 wt/vol %).

copolymer, and the IEP is never observed. Micelles are detected at low pHs while small aggregates are once again observed at high pHs. That electrostatic interactions are built up at high pHs is confirmed by redissolution upon addition of salt and Debye screening (data at pH = 10 in Table 3). The small aggregates are thought to be soluble complexes of positively and negatively charged blocks.[25]

Figure 4 shows how R_h, determined by the Stokes–Einstein equation, depends on pH for the PMAA(49)-*b*-PDMAEMA(11) sample. The data are quite comparable to previously reported DLS experiments for PMAA-*b*-PDMAEMA copolymers of quite the same composition but of higher molecular weight.[26] At pHs lower than 4, micelles are observed by DLS, which would consist of an essentially uncharged PMAA core, surrounded by a

Table 3. Effect of Salt on the Hydrodynamic Radius R_h of the Aggregates Formed by the Quaternized PMAA(15)-*b*-PDMAEMA(120) Copolymer at pH = 4 and pH = 10 (C = 0.01 wt/vol %)[a]

NaCl concn (mol/L)	R_h at pH = 4 (nm)	R_h at pH = 10 (nm)
0.1	141	7 + uns
0.25	135	7 + uns
0.5	122	7 + uns
1	113	248

[a] Uns = presence of unsoluble material.

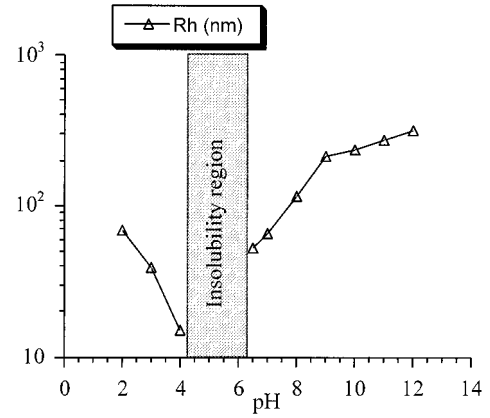

Figure 4. Hydrodynamic radius of the PMAA(49)-*b*-PDMAEMA(11) copolymer as a function of pH (C = 0.01 wt/vol %).

corona of protonated PDMAEMA blocks. The size of these micelles is rather large and the polydispersity as well. Figure 5a shows the CONTIN distribution for this copolymer at pH = 2. As the pH is increased (2 < pH < 5), the size of the micelles decreases (Figure 5b). This effect should be related to electrostatic interactions between positively charged PDMAEMA and negatively charged PMAA segments, as it will be discussed in the next section. Indeed, the pK_a of MAA being 5.35, a significant amount of MAA units should be ionized at pH = 5. The IEP is localized at pH ranging between 5 and 6.5 (Table 1), in relation to the copolymer insolubility.

Above pH = 6.5, the PMAA(49)-*b*-PDMAEMA(11) copolymer is again soluble, and the R_h of the micelles increases with pH, micelles of ca. 250 nm being detected at pH = 10. The CONTIN size distribution of the micelles at pH = 7, 9, and 10 is shown in parts c, d, and e of Figure 5, respectively. It is clear that at least two populations of aggregates coexist in this pH range, since small micelles coexist with larger aggregates. The large aggregates dominate the system at high pH, and their size and size polydispersity increase with the pH. The same observation was previously reported by size exclusion chromatography of aqueous solutions of PMAA-*b*-PDMAEMA block copolymers at pH = 9.[24] Some of us noted the coexistence of unimers and a series of aggregated species.

The effect of salt on the size of the micelles formed by the PMAA(49)-*b*-PDMAEMA(11) copolymer at three different pHs has been investigated. The results are shown in Table 4. The addition of salt to ampholytic copolymers may have a priori two opposite consequences, i.e., the screening of the electrostatic charges which may cause the dissolution of the aggregates at and above a critical salt concentration and a salting-out effect which would decrease the solubility and lead to flocculation. The Debye screening effect is expected to dominate in the case of electrostatically driven aggregation. It is indeed what happens in the pH range of the IEP since the copolymer is redissolved upon salt addition (Table 4). At pHs below or above the IEP, the salt has no significant effect on the size of the aggregates, at least under the investigated conditions.

Table 4. Effect of Salt on the Hydrodynamic Radius of the Aggregates Formed by the PMAA(49)-*b*-PDMAEMA(11) Copolymer at pH = 4, 6, and 10 (C = 0.01 wt/vol %)[a]

NaCl concn (mol/L)	R_h at pH = 4 (nm)	R_h at pH = 6 (nm)	R_h at pH = 10 (nm)
0.1	17	uns	240
0.25	21	uns	255
0.5	17	453	253
1	15	377	277

[a] Uns = presence of unsoluble material.

The PDMAEMA block of the PMAA(49)-*b*-PDMAEMA(11) copolymer has been quaternized by iodomethane, which provides the copolymer with a permanent positive charge insensitive to pH and well-suited to the probing of the electrostatic interactions. The quaternized copolymer has been analyzed by DLS as a function of pH (Figure 6) and salt concentration. At pH below 5, the quaternized copolymer behaves similarly to the non-quaternized parent compound. At high pHs, the copolymer is insoluble, and no DLS measurement can be done. A partial dissolution is however observed upon salt addition, which is reminiscent of mixtures of oppositely charged homopolyelectrolytes. In this respect, stoichiometric complexes of oppositely charged homopolyelectrolytes (coacervates) form unstable aggregates in aqueous solution and phase separate.[27] Nonstoichiometric complexes are however stabilized by uncompensated charge and may remain soluble.[25] The stability and size of these complexes depend on how important are the uncompensated charge and the ionic strength. The quaternized PMAA(49)-*b*-PDMAEMA(11) is thought to form quite similar complexes, whose the solubility is improved by salt addition. Similar observations have been reported for samples containing a major PDMAEMA block in which soluble nonstoichiometric complexes are thought to be formed at high pHs.

Transmission Electron Microscopy. The morphology of PMAA-*b*-PDMAEMA diblocks has been analyzed by TEM as a function of pH. Samples containing a major PDMAEMA block form spherical micelles below the IEP, which are shown for the PMAA(15)-*b*-PDMAEMA(120) copolymer in Figure 7. Quite similar morphology is observed for samples containing a major PMAA block below the IEP, as shown in Figure 8a for the PMAA(49)-*b*-PDMAEMA(11) copolymer. At pH above the IEP, aggregates were detected by DLS, and the size of these aggregates was observed to increase with pH. Their morphology observed by TEM is however quite surprising. Indeed, at pH = 6.8, hollow aggregates are clearly observed, whose size increases with pH (Figure 8b−d). In some cases, small spherical micelles coexist with these unusual hollow aggregates (Figure 8c). These apparently hollow aggregates are thought to be originally filled with solvent which has not been removed during the lyophilization process (some of them are visible in Figure 8b). Actually, upon electron beam irradiation, one can clearly see the solvent boiling and leaving the aggregates empty.

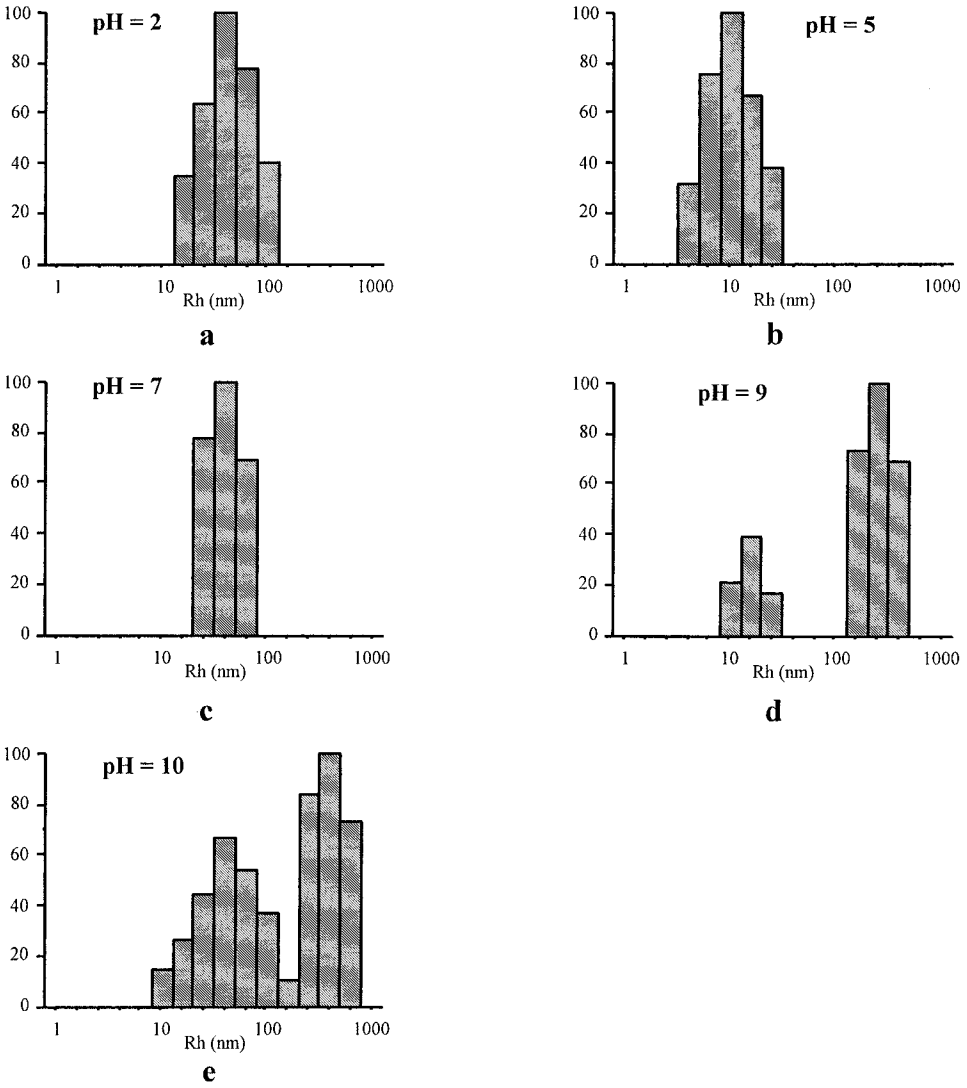

Figure 5. CONTIN size distribution for the PMAA(49)-*b*-PDMAEMA(11) copolymer at pH = 3 (a), 5 (b), 7 (c), 9 (d), and 10 (e) (C = 0.01 wt/vol %).

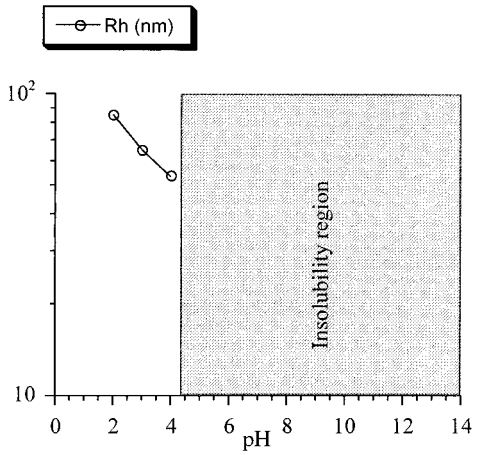

Figure 6. Hydrodynamic radius of the quaternized PMAA-(49)-*b*-PDMAEMA(11) copolymer as a function of pH (C = 0.01 wt/vol %).

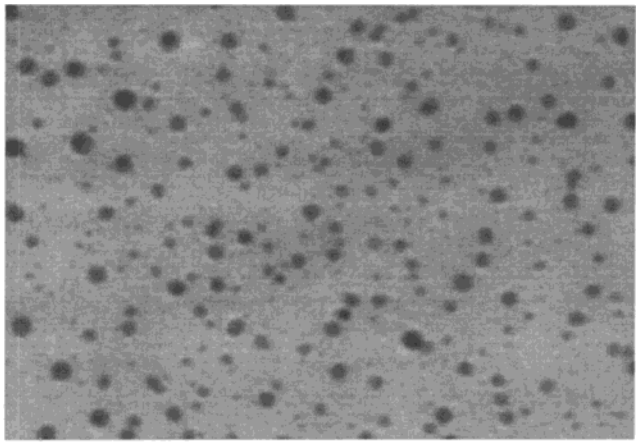

Figure 7. Micelles observed by TEM in the PMAA(15)-*b*-PDMAEMA(120) copolymer at pH = 4 (C = 0.01 wt/vol %).

At higher pH, further aggregation takes place, which results from the tendency of the hollow aggregates to form much larger complex multicompartmentalized aggregates. Some of these internal compartments are still filled with solvent that evaporates upon observation and leads to some breaking of the internal walls. The whole size of these superaggregates as well as the size of the internal compartments increases with increasing pH, as proved by comparison of parts e and f of Figure 8. So, TEM observations are quite consistent with the previously reported DLS data.

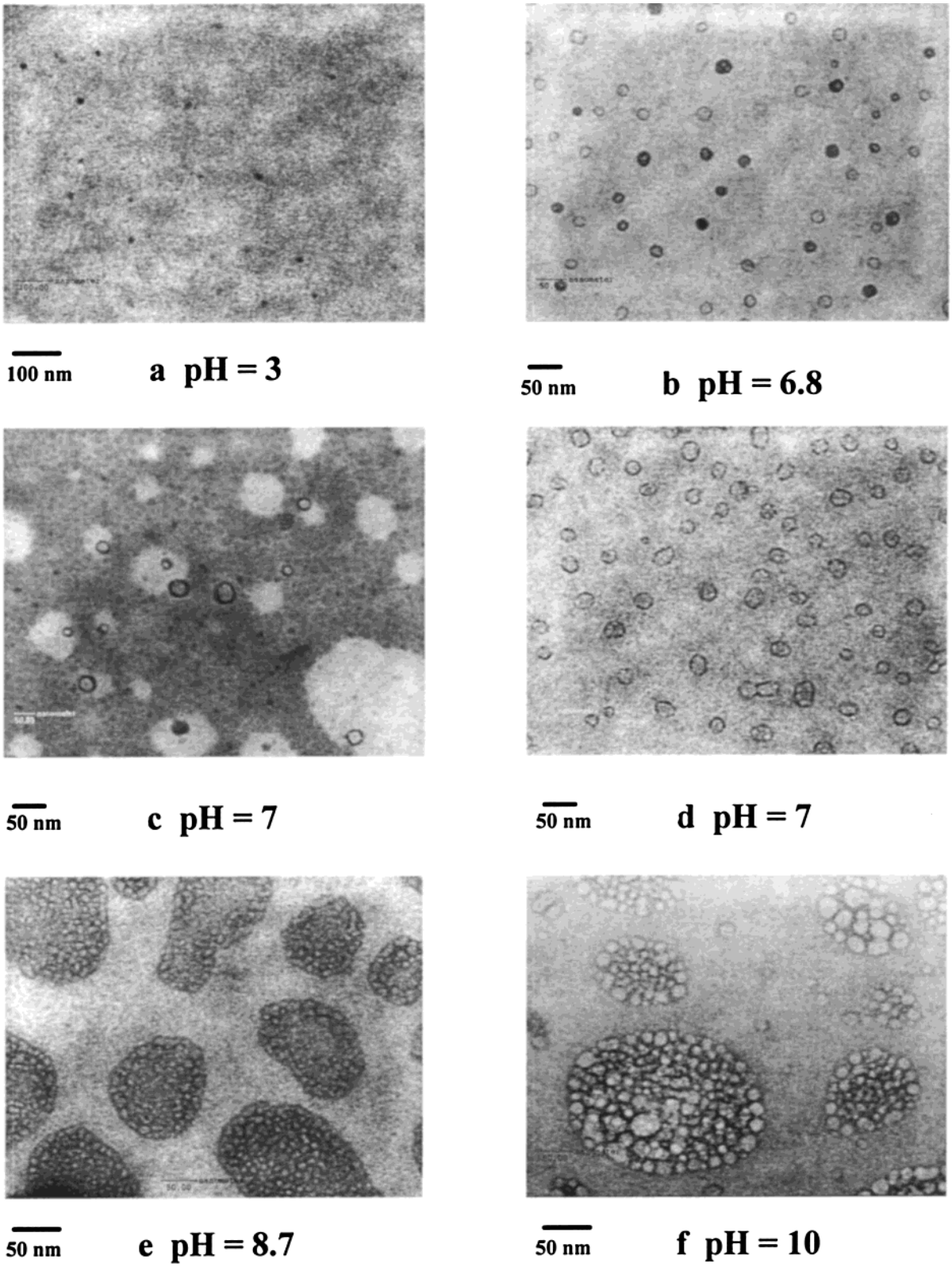

Figure 8. TEM pictures of the aggregates formed by the PMAA(49)-*b*-PDMAEMA(11) copolymer as a function of pH (C = 0.01 wt/vol %).

The formation of vesicle-like aggregates has also been confirmed by cryo-TEM of concentrated copolymer solution (10 wt/vol %) as shown in Figure 9. The cryo-TEM technique is well-suited to the observation of these soft biomimetic materials since the chance of perturbing the actual structures in solution is minimized. The cryo-TEM picture of Figure 9 clearly shows vesicle structures formed by the PMAA(49)-*b*-PDMAEMA(23) copolymer at pH = 9. These vesicles are not aggregated as was observed by TEM in the low concentration regime. Their diameter is comparable to the size measured by DLS and TEM at low concentration. The thickness of the vesicle membrane has been estimated at ca. 10 nm in Figure 9, which is consistent with a bilayer formed by the stretched short PDMAEMA blocks of the PMAA-(49)-*b*-PDMAEMA(23) copolymer.

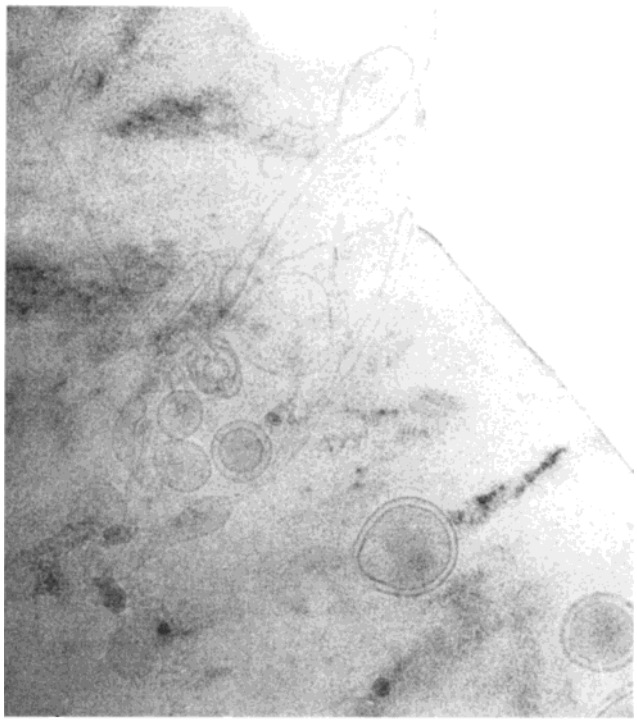

Figure 9. Aggregates observed by cryo-TEM in the PMAA-(49)-*b*-PDMAEMA(23) copolymer at pH = 9 (C = 10 wt/vol %).

Table 5. I_1/I_3 Ratio for the PMAA-*b*-PDMAEMA Copolymers at Different pH Values (C = 0.01 wt/vol %)

pH	I_1/I_3 ratio for PMAA(49)-*b*-PDMAEMA(11) copolymer	I_1/I_3 ratio for PMAA(51)-*b*-PDMAEMA(109) copolymer
3	0.96	0.97
6	1.13	1.01
8	0.93	1.15
10	0.9	1.08
12	0.85	0.98

Fluorescence Spectroscopy. Pyrene has been used to probe the internal structure of the core of the micelles. The emission spectrum of pyrene depends indeed on the environment, the third peak being more intense (I_3) than the first peak (I_1) in a hydrophobic environment.[28] The experimental values of I_1/I_3 depend on the wavelength of the excitation light,[29] and they are biased toward low values when λ_{ex} is 339 nm and toward high values at 333 nm. At λ_{ex} = 335 nm used in this study, the I_1/I_3 ratio should be equally weighted for the two states.[30] For the sake of comparison, the I_1/I_3 ratio is ca. 1.8−2.0 in pure water depending on temperature, whereas it decreases in the range from 0.95[23] to 1.5[28,31] in the hydrophobic environment of micellar core. The I_1/I_3 ratio has been measured for the PMAA(49)-*b*-PDMAEMA(11) and PMAA(51)-*b*-PDMAEMA(109) copolymers as a function of pH, as reported in Table 5. This ratio passes through a maximum in the vicinity of the IEP when the pH is increased. At low pH, the polymethacrylate backbone of the unsoluble polyacid block forms hydrophobic domains. At pH close to the IEP, the complexation of the two blocks into polysalt changes the environment for the pyrene which appears to be more water friendly or, at least, more hydrophilic. At high pH, the uncharged PDMAEMA block would host pyrene in a more hydrophobic environment. The I_1/I_3 values observed for the micellar solutions considered in this study are in complete agreement with those ones recently reported for micelles formed in water by poly(2-(dimethylamino)methyl methacrylate)-*b*-poly(2-(diethylamino)methyl methacrylate) diblocks.[23]

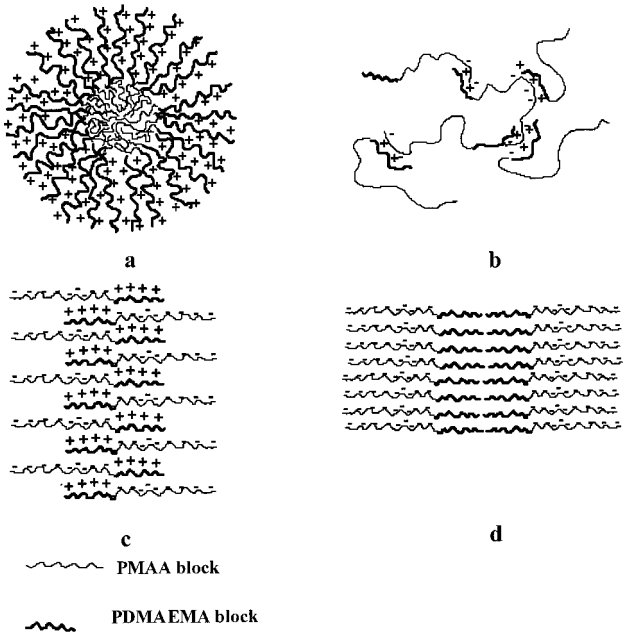

Figure 10. Sketches of the association models for PMAA-*b*-PDMAEMA copolymers.

Discussion. The experimental data collected in this study show that two different driving forces operate in the supramolecular organization of amphoteric diblock copolymers, i.e., electrostatic interaction between positively and negatively charged units and hydrophobic interaction. It has been shown in the scientific literature that these two processes can be at the origin of molecular aggregation.[1,11,12,25,27,32]

At pHs below the IEP, spherical micelles are formed as result of hydrophobic interaction of the uncharged PMAA blocks in water, independent of the relative length of the constituent PDMAEMA blocks. The association model is shown in Figure 10a. At increasing pH, part of the PMAA blocks is ionized, and electrostatic interactions between these negative units and the positively charged PDMAEMA blocks occur together with a decrease in the size of the micelles (Figure 4). This modification in size reflects a change in the structure of the core as pH is increased. The polysalt formed by the association of the oppositely charged blocks should be incorporated in the core, as reported by Kataoka et al.,[11,32b,c] Kabanov et al.,[32a] and Cohen-Stuart et al.[12] In these studies, the resulting aggregates were soluble because the charged blocks were associated with water-soluble nonionic blocks. For the copolymers considered in this study, the excess of positive charges at pH below the IEP contributes to the stability of the micellar solution. As pH is increased closer to the IEP, the core of the micelles increasingly consists of compact polysalt. In parallel, the uncompensated positive charge decreases and the micelle stability as well. Actually, the micelles are thought to reorganize into small-size soluble polyelectrolyte-like complexes, stabilized by the excess of positively charged units, as happens in the case of nonstoichiometric mixtures of oppositely charged polyelectrolytes.[25]

At the IEP, the strong electrostatic interactions between the oppositely charged blocks dominates, and

the lack of uncompensated free charges results in the insolubility of the copolymer (Figure 4). The association model is shown in Figure 10b. The system is basically the same as stoichiometric mixtures of oppositely charged polyelectrolytes.[27] These electrostatic interactions can however be screened by a salt that can restore the solubility (Tables 3 and 4). This aggregation regime persists at pH higher than the IEP for copolymers containing a major PDMAEMA block, the uncompensated negative charge being unable to stabilize the aggregated species. For the PMAA(15)-*b*-PDMAEMA-(120) copolymer, small-size soluble polyelectrolyte complexes however coexist with the insoluble material at and above the IEP (Figure 1).

An additional aggregation regime is observed for copolymers containing a major PMAA block, since, above the IEP, the copolymer is again soluble and quite unexpected morphologies are observed by TEM. In this respect, it is worth recalling that the pK_a of DMAEMA is 8[14] and that one of PMAA is 5.35.[20] Therefore, above the IEP (ca. pH = 5 for the PMAA(49)-*b*-PDMAEMA-(11) copolymer), most of the PMAA units are ionized in contrast to the ionization of the PDMAEMA units which is only partial. Two models can be proposed for the aggregation of the copolymer chain in this pH range (Figure 10c,d). The first model relies on the electrostatic interaction of the oppositely charged blocks, the uncompensated negative charges of the PMAA units stabilizing the aggregates. The second model is based on the hydrophobic interaction of the noncharged PDMAEMA blocks (Figure 10d) and should be as valid as the pH is high. Actually, the two aggregation modes may coexist, the electrostatic interactions being gradually replaced by hydrophobic ones at increasing pH with the concomitant release of the negatively charged MAA units from the micellar core. This reorganization is in complete agreement with the fluorescence spectroscopy measurements, which indicated that the hydrophobicity of the core was increasing with pH above the IEP. It may be surprising that the nonprotonated PDMAEMA blocks contribute to hydrophobic interaction since this homopolymer is usually considered to be soluble in water, even at high pH.[23] However, the cloud point temperature for uncharged PDMAEMA homopolymer in water has been reported to be in the range 32-46 °C depending on the molecular weight.[33] So the cloud point would be shifted toward lower temperature when PDMAEMA is chemically bonded to an ionized PMAA block, more likely as a result of punctual intramolecular repulsion. This conclusion is in apparent contradiction with a previous paper, according to which same type of PMAA-*b*-PDMAEMA copolymers do not form micelles at room temperature but large aggregates of ca. 400 nm at 50 °C and pH = 9.5.[33] However, most of these copolymers contained a major PDMAEMA block. Nevertheless, precipitation driven by hydrophobic interaction has been observed in this study for diblocks containing a major PDMAEMA block at high pH. So, it seems that the cloud point of the DMAEMA block is reached at room temperature for all the copolymers considered in this study. Finally, it should be pointed out that the formation of micelles by PMAA-*b*-PDMAEMA diblocks in water at room temperature has been reported elsewhere.[24,26] Moreover, all the experiments of this study have been carried out in the presence of phosphate buffer salt. The ionic strength of the solution could have a strong influence on the hydrophobicity (hydrophilicity) of the nonprotonated PDMAEMA block.

Two questions are still pending. Why are hollow aggregates formed instead of spherical micelles? Why do these hollow aggregates further associate into multicompartmentalized superaggregates? The first question can be answered on the basis of elementary geometrical and free energy considerations. In micelles, the unsoluble block is usually stretched to an extent that however depends on the geometry of the core. Since this structuring causes an entropy penalty, the micelles will adopt themselves to the most favorable geometry. In this respect, Eisenberg and Zhang[4] have shown that the stretching of the insoluble polystyrene block of polystyrene-*b*-poly(acrylic acid) diblocks in water was considerably larger in spherical micelles (the ratio of the core radius to the chain end-to-end distance in the unperturbed state being 1.4) than in rodlike micelles (ratio = 1.25) and than in vesicles or lamellae (ratio = 1.0). This general tendency could actually explain the formation of the hollow aggregates by the PMAA-*b*-PDMAEMA copolymers containing a short noncharged PDMAEMA block and a longer ionized PMAA one. If the copolymer molecules are assumed to be packed in a bilayer fashion as schematized in Figure 10d, an important free energy penalty should result from the bending of the bilayer in order to form the hollow aggregates of a rather small diameter (Figure 8). Nevertheless, classical vesicles are usually prepared from bilayer structures which are further bent by an external input of mechanical energy. Therefore, the hollow aggregates must be regarded as a rather unstable organization. In the following, the evolution of the morphologies are tentatively explained by the coalescence of these unstable hollow aggregates into much bigger structures, as the pH is increased. In a first step, the individual hollow aggregates merge together to form multicompartmentalized structures (Figure 8e). Then, the internal walls break up with formation of larger vesicle type substructures, which remain aggregated (Figure 8f). This modification of the structure, which requires that the system overcome the electrostatic repulsion of the charged PMAA corona of the original small hollow aggregates, results in the decrease of the bending energy. There are some similarities in this process and endocytosis, which is characterized by the merging of two negatively charged phospholipid-containing bilayers.[34] The supramolecular organization of the system changes as the pH is increased and thus as the electrostatic interactions between oppositely charged PDMAEMA and PMAA blocks in the core are replaced by hydrophobic ones between uncharged PDMAEMA blocks. The transition from the electrostatic interactions to the hydrophobic ones triggers a parallel transition from a dense core of polyelectrolyte complexes surrounded by water-soluble blocks of PMAA to hydrophobic microdomains of PDMAEMA in which the stretching of these constituent blocks is restricted by the suborganization of the diblocks in lamellae structures. The size of the water-soluble blocks increases as they are released from the polyelectrolyte complexes. At increasing pH (>7.5), the system tends to minimize the bending energy of the lamellae by the merging of the individual hollow aggregates into larger structures. At this point, it is not clear yet whether the morphologies observed at different pHs are at the thermodynamic equilibrium or they are kinetically controlled.

Conclusions

The self-association of PMAA-*b*-PDMAEMA amphoteric diblocks copolymers in water has been studied as a function of copolymer composition, pH, and salt concentration. Three different association regimes have been identified. At pH below the IEP, spherical micelles consisting of a noncharged PMAA block surrounded by a positively charged PDMAEMA corona are formed. As pH is increased, part of the MAA units are ionized, which form polyelectrolyte complexes with positively charged PDMAEMA. These intrinsically insoluble complexes are part of the cores of the micelles and cause a decrease of their size. No precipitation occurs because the uncompensate positive charge of the PDMAEMA blocks maintain the insoluble component in solution. Close to the IEP, electrostatic interaction of the constituent blocks and the lack of net charges on one of them results in the insolubility of the copolymer. These electrostatic interactions can however be screened by a salt. For copolymers that contain a major PMAA block, soluble aggregates are formed at pHs higher than the IEP. The ionization of the PDMAEMA blocks then decreases rapidly so that the hydrophobic interaction of these blocks dominates at the expense of the electrostatic interaction with the PMAA blocks. The diblocks then self-organize into vesicle-like structures in order to minimize the chain stretching of the PDMAEMA blocks. For this reason, the accordingly formed small hollow aggregates tend to merge into much larger multicompartmentalized aggregates.

Acknowledgment. J.F.G. and R.J. are very much indebted to the "Services Fédéraux des Affaires Scientifiques, Techniques et Culturelles" for financial support in the frame of the "Pôles d'attraction Interuniversitaires: 4-11: Chimie Supramoléculaire et Catalyse Supramoléculaire". The authors are grateful to P. Bomans and P. M. Frederik (State University of Limburg, Maastricht) for the cryo-TEM observations and to M. Dejeneffe (CERM, Liège) for her skillful technical assistance.

References and Notes

(1) (a) Tuzar, Z.; Krachtovil, P. *Surface and Colloid Science*; Matijevic, E., Ed.; Plenum Press: New York, 1993. (b) Chu, B. *Langmuir* **1995**, *11*, 414. (c) Alexandridis, P. *Curr. Opin. Colloid Interface Sci.* **1996**, *1*, 490. (d) Selb, J.; Gallot, Y. In *Developments in Block Copolymers*; Goodman, I., Ed.; Elsevier: Amsterdam, 1985; Vol. 2, p 85. (e) Moffit, M.; Khougaz, K.; Eisenberg, A. *Acc. Chem. Res.* **1996**, *29*, 95.
(2) Förster, S.; Zizenis, M.; Wenz, E.; Antonietti, M. *J. Chem. Phys.* **1996**, *104*, 9956.
(3) Israelachvili, J. N. *Intermolecular and Surface forces*; Academic Press: London, 1985.
(4) Zhang, L.; Eisenberg, A. *Science* **1995**, *268*, 1728.
(5) (a) Zhang, L.; Eisenberg, A. *J. Am. Chem. Soc.* **1996**, *118*, 3168. (b) Zhang, L.; Yu, K.; Eisenberg, A. *Science* **1996**, *272*, 1777. (c) Zhang, L.; Shen, H.; Eisenberg, A. *Macromolecules* **1997**, *30*, 1001. (d) Zhang, L.; Eisenberg, A. *Macromolecules* **1996**, *29*, 8805. (e) Yu, K.; Eisenberg, A. *Macromolecules* **1996**, *29*, 6359. (f) Yu, K.; Eisenberg, A. *Macromolecules* **1998**, *31*, 3509. (g) Yu, Y.; Zhang, L.; Eisenberg, A. *Macromolecules* **1998**, *31*, 1144. (h) Yu, Y.; Zhang, L.; Eisenberg, A. *Langmuir* **1997**, *13*, 2578. (i) Shen, H.; Zhang, L.; Eisenberg, A. *J. Phys. Chem.* **1997**, *101*, 4697. (j) Yu, K.; Zhang, L.; Eisenberg, A. *Langmuir* **1996**, *12*, 5980. (k) Yu, Y.; Eisenberg, A. *J. Am. Chem. Soc.* **1997**, *119*, 8383. (l) Yu, G.; Eisenberg, A. *Macromolecules* **1998**, *31*, 5546.
(6) Ding, J.; Liu, G. *Macromolecules* **1997**, *30*, 655.
(7) Ding, J.; Liu, G. *Chem. Mater.* **1998**, *10*, 537.
(8) (a) Jenekhe, S. A.; Chen, X. L. *Science* **1998**, *279*, 1903. (b) Jenekhe, S. A.; Chen, X. L. *Science* **1999**, *283*, 372.
(9) Cornelissen, J. J.; Fischer, M.; Sommerdijk, N. A.; Nolte, R. J. *Science* **1998**, *280*, 1427.
(10) Discher, B. M.; Won, Y. Y.; Ege, D. S.; Lee, J. C. M.; Bates, F. S.; Discher, D. E.; Hammer, D. A. *Science* **1999**, *284*, 1143.
(11) Harada, A.; Kataoka, K. *Science* **1999**, *283*, 65.
(12) Cohen Stuart, M. A.; Besseling, N. A. M.; Fokkink, R. G. *Langmuir* **1998**, *14*, 6846.
(13) Creutz, S.; Teyssié, P.; Jérôme, R. *Macromolecules* **1997**, *30*, 6.
(14) Patrickios, C. S.; Hertler, W. R.; Abbott, N. L.; Hatton, T. A. *Macromolecules* **1994**, *27*, 930.
(15) Tanford, C. *Physical Chemistry of Macromolecules*; Wiley: New York, 1961.
(16) Velick, S. F. *J. Phys. Colloid Chem.* **1949**, *53*, 135.
(17) Healy, T. W.; Homola, A.; James, R. O.; Hunter, R. *J. Faraday Discuss. Chem. Soc.* **1978**, *65*, 156.
(18) Erlich, G.; Doty, P. *J. Am. Chem. Soc.* **1954**, *76*, 3764.
(19) Mazur, J.; Silberberg, A.; Katchalsky, A. *J. Polym. Sci.* **1959**, *35*, 43.
(20) Merle, Y. *J. Phys. Chem.* **1987**, *91*, 3092.
(21) Pradny, M.; Seveik, S. *Makromol. Chem.* **1985**, *186*, 111.
(22) Merle, Y. *J. Phys. Chem.* **1987**, *91*, 3092.
(23) Lee, A. S.; Gast, A.; Bütün, V.; Armes, S. P. *Macromolecules* **1999**, *32*, 4302.
(24) Creutz, S.; van Stam, J.; De Schrijver, F. C.; Jérôme, R. *Macromolecules* **1998**, *31*, 681.
(25) Zezin, A. B.; Kabanov, V. Russ. *Chem. Rev. (Engl. Transl.)* **1982**, *51*, 833.
(26) Walter, H.; Harrats, C.; Müller-Buschbaum, P.; Jérôme, R.; Stamm, M. *Langmuir* **1999**, *15*, 1260.
(27) (a) Tsuchida, E.; Abe, K. *Adv. Polym. Sci.* **1982**, *45*, 2. (b) Dautzenberg, H.; Jaeger, W.; Kötz, J.; Philipp, B.; Seidel, Ch., Stscherbina, D. In *Polyelectrolytes, Formation, Characterization and Application*; Hanser Publisher: Munich, 1994; Chapter 6.
(28) Chen, W. Y.; Alexandridis, P.; Su, C. K.; Patrickios, C. S.; Hertler, W. R.; Hatton, T. A. *Macromolecules* **1995**, *28*, 8604.
(29) (a) Zhao, C. L.; Winnik, M. A.; Riess, G.; Croucher, M. D. *Langmuir* **1990**, *6*, 514 (b) Wilhem, M.; Zhao, C. L.; Wang, Y.; Xu, R.; Winnik, M. A.; Mura, J. L.; Riess, G.; Croucher, M. D. *Macromolecules* **1991**, *24*, 1033.
(30) Anthony, O.; Zana, R. *Macromolecules* **1994**, *27*, 3885.
(31) Nivaggioli, T.; Alexandridis, P.; Hatton, T. A.; Yekta, A.; Winnik, M. A. *Langmuir* **1995**, *11*, 730.
(32) (a) Kabanov, A. V.; Bronich, T. K.; Kabanov, V. A.; Yu, K.; Eisenberg, A. *Macromolecules* **1996**, *29*, 6797. (b) Harada, A.; Kataoka, K. *Macromolecules* **1998**, *31*, 288. (c) Kataoka, K.; Togawa, H.; Harada, A.; Yasugi, K.; Matsumoto, T.; Katayose, S. *Macromolecules* **1995**, *28*, 5294.
(33) Lowe, A. B.; Billingham, N. C.; Armes, S. P. *Chem. Commun.* **1997**, 1035.
(34) de Duve, C. *A Guided Tour of The Living Cell*; W. H. Freeman and Co.: New York, 1984.

MA992016J